Influence of Vibrations on Interface Delamination in Metal–Polymer Composites

E. Zumelzu,[1] R. Pereira,[2] J. P. Arenas,[2] F. Rull,[3] R. Silva[4]

[1]Instituto de Materiales y Procesos Termomecánicos, Universidad Austral de Chile, Casilla 567, Valdivia, Chile
[2]Instituto de Acústica, Facultad de Ciencias de la Ingeniería, Universidad Austral de Chile, Valdivia, Chile
[3]Departmento Física de la Materia Condensada, Universidad de Valladolid, Valladolid, Spain
[4]Unidad de Microscopia Electrónica, Universidad Austral de Chile, Valdivia, Chile

ABSTRACT: The main objective of this work was the study of vibration effects on the viscoelastic coating protecting the steel layer in a metal–polymer composite, with simulated conditions of the transportation of food containers. Mechanical resonance tests in metal–polymer [electrolytic chromium-coated steel–poly(ethylene terephthalate) (PET)] sheets were performed to generate vibration conditions to induce structural modifications in the viscoelastic layer covering the surface of the plates. Consequently, schematic representations of the areas affected by these modifications were made. The modified structures were later analyzed by electron microscopy to detect and evaluate alterations in the morphology of the material. In addition, vibrational Raman spectroscopy analyses were performed to assess the chemical and structural changes on the protective PET at the metal–polymer interface level. The results of this study are expected to provide basic information on the mechanisms and nature of the delamination processes taking place in metal–polymer laminates employed in food-container applications. These damages have previously been detected in some food containers made of PET materials. The study of these damages can lead to the improvement of current composites or the development of higher quality materials. © 2011 Wiley Periodicals, Inc. J Appl Polym Sci 125: 97–103, 2012

Key words: adhesion; coatings; composites; electron microscopy; Raman spectroscopy

INTRODUCTION

Manufacturers of food containers are highly concerned with the delamination problems encountered in metal–polymer laminates, especially in electrolytic chromium-coated steel (ECCS) surfaces protected by poly(ethylene terephthalate) (PET) copolymers. This composite material has been characterized as an advanced, knowledge-intensive, and multifunctional material because of its properties of adhesion and corrosion resistance.[1]

The PET coating is employed as a laminated material because of its high-quality mechanical properties, good adhesion to steel, and low permeability to water.[2,3] The incorporation of a comonomer produces the component with a lower fusion temperature and, therefore, reduces the rolling temperature during manufacturing.[4,5] In addition, the application of a controlled thermal treatment results in a multilayer composite with various microstructures, which determine the ultimate mechanical properties of the material during the thermomechanical processes of manufacturing.

On the other hand, the metal substrate of the material is composed of a base made of steel and an electrolytic fine coating that protects the steel and allows good adherence of the protective PET polymer. The electrolytic layer is formed by metal chromium and chromium oxides, with an average content of 80 mg/m^2 metal chrome and 20 mg/m^2 chromium oxides. Figure 1 shows the schematic representation of the laminated metal–polymer.

The outer layer of chromium oxide on the steel interacts with the polymer coating to produce a protective barrier system against the aggressive media; this results in a strong chemical adhesion of the substrates at the interface level.

To evaluate the structural integrity of the composite, analyses of adherence of the different substrates are performed; this information is useful for foreseeing the behavior in different applications after the forming process. The ability to measure the adhesion of the coating to the metal substrate by the employment of different methods, such as the elcometer pull-off, blistering, T-peeling, or variable radius roll adhesion testing, is a key factor in ensuring the quality and development of products and comparison of different coating–substrate systems.[6–9]
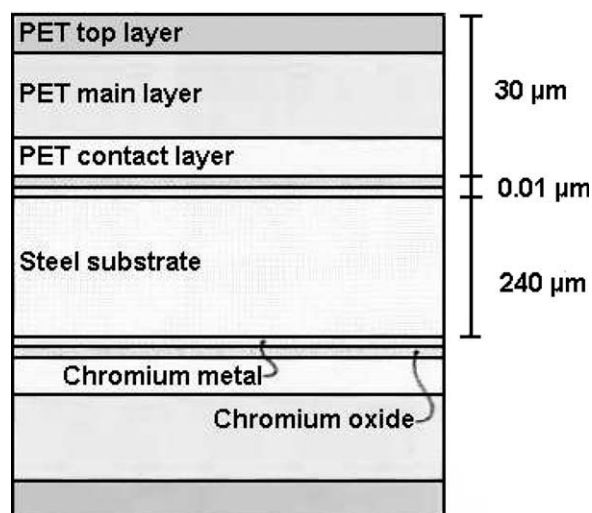
Figure 1 Cross section of a laminated metal–polymer composite.

All of these trials are commonly used to evaluate the adherence of substrates in the manufacturing of metal–polymer plates, after the formation of containers or recipients, and during their useful life in these applications.

Mechanical resonance occurs when the frequency of the applied vibration force is coincident with the natural frequencies of the system on which it acts. Under these circumstances, the system vibrates, progressively increasing the amplitude of the oscillatory motion after each of the successive applications of force. Thus, the resonance can induce destructive effects on the morphology of the body involved.[10] The natural frequencies are generally functions of the boundary conditions on the mechanical system, the system geometry, and its material properties.

When in resonance, a body vibrates and acquires particular characteristics called *modes of vibration*. Each mode of vibration is characterized by the definite appearance of points of no displacement (nodes) and points of maximum displacement (antinodes) during each vibration cycle of a particular mode. This observable fact, also known as a *standing wave pattern*, is originated by the interference resulting from the presence of two bending waves of the same frequency with different travel directions in the body.

Several theoretical and experimental studies have been carried out to determine the corresponding natural frequencies and modes of vibration in plates.[11–17] For the correct prediction of the behavior of the system at resonance, it is necessary to know the different structural parameters of the system under study.[18–22] If these parameters are not known, the application of experimental methods is necessary.

In this work, we approached the study of some original aspects concerning the vibration effects on visco-elastic PET coatings that protect thin, ECCS plates in food-container applications. It is possible that the resonance vibrations may damage the PET substrate adhesion to the steel, particularly at points corresponding to a vibration antinode, when the conditions of marine transport of containers are simulated. Thus, a controlled experimental procedure devised to produce surface damage in metal–polymer samples is presented here. In the technical literature, to the best of our knowledge, no vibration test has been reported to detect microscopic delamination.

EXPERIMENTAL

In our experimental study, we considered the design and implementation of a measurement system for the determination of frequency response functions, acceleration, and force signals needed for the modal analysis of vibrations. The plates under study were subjected to bending by means of an electrodynamic vibration shaker. The mechanical resonance condition forced the generation of standing wave patterns in the sample. The former allowed detection of the areas undergoing maximum displacement.[23]

The measurement system consisted of a computer-controlled signal-capture analog-to-digital (A/D) NI PCI-6036E card and software implemented in Lab-View. The measurements were performed with a small vibration sensor (PCB 352C22 accelerometer, 0.5 g) powered by a signal conditioner (PCB 480C02), an electrodynamic shaker (B&K 4810), an equalizer (Behringer FBQ 6200, Willich, Germany), and a pure-tone signal generator (B&K 1022). The data analyses were made by software developed in MatLab R12. The experimental studies considered seven samples of metal–polymer sheets 21 × 13.5 cm² in size. The system was calibrated before each test by a B&K 4294 vibration calibrator driven by a crystal oscillator that provided a constant acceleration of 9.8 m/s² at a frequency of 159.15 Hz (1000 rad/s).

A strong metallic frame to simulate a clamped perimeter was built for the vibration experiments. The reason for this design was the high flexibility of the plates under study, which prevented the implementation of standard systems, such as that, for example, of the free-clamped beam. The frame made it possible to reach the stability required for the application of forces and the continuous and steady-state excitation of the vibration modes. Both uniformity and adhesion of the coating were previously ensured for all of the samples subjected to the vibration tests.

The measurement and analysis procedure consisted of acquiring the signals from the vibration sensor attached to the metal–polymer plate, which was excited by an electrodynamic shaker. The process of identification of resonances implied the application of a thin layer of fine powder to the
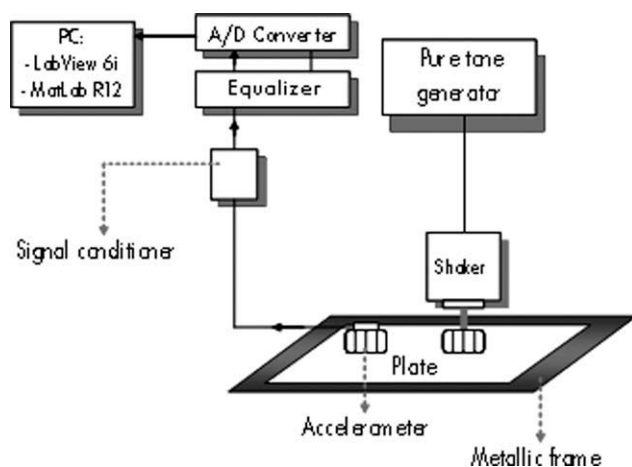
Figure 2 Experimental setup for the vibration analyses (PC = personal computer).

surface of the samples because of their extreme flexibility. Then, they were submitted to a continuous frequency scanning excitation until a definite vibration mode was reached. After that, each sample was exposed to the resonance condition during a time fluctuating between 1 h 30 min and 3 h. Under these conditions, acceleration measurements at 15 different points on the plate were performed. The required antinode points were determined through bidimensional interpolation routines implemented in MatLab R12 with the values of acceleration recorded at the 15 points of every plate. Figure 2 shows the experimental setup.

During the experimental trials, all of the measured data were stored for subsequent analyses. These analyses allowed the determination of detachment areas, which were later evaluated by scanning electron microscopy (SEM), and Quanta three-dimensional dual beams for PET observations.

Raman and micro-Raman vibration spectroscopy analyses were performed at parallel intervals from the surface to the metal interface to characterize the rutile distribution in the PET thickness to determine the influence on the antinodes areas or zones with chemical and structural alterations.

This part of the study employed the following Raman devices: a Kaiser Holospec f/1.8i spectrometer (Ann Arbor, Michigan), with a spectrum range of 100–3800 cm^{-1} and a resolution of 4 cm^{-1}; an Andor DV420A-OE-130 charged coupling device; and a laser Melles-Griot 0.5-lhp-151 (He–Ne 632.8 nm). We macroanalyzed the samples by making the laser beam strike perpendicular to the surface with a Raman of 785 nm. Also, cross sections of the samples were microanalyzed parallel to the coating by means of the Raman device at 633 nm, obtaining spectra every 5 μm at different points starting from the PET surface until the ECCS interface was reached. The diameter of the laser spot was approximately 10 μm.

The measurements and characterizations were used to correlate these points with the possible effect on the delamination and to verify the presence of defects and discontinuities at the metal–polymer interface commonly seen in the coextrusion manufacturing process of PET-coated ECCS sheets.

RESULTS AND DISCUSSION

Figure 3(1) summarizes the results obtained from the antinode zones detected during the experiments. This figure shows the presence of a well-defined node line along the plate and indicates two zones of maximum displacement along the sheet. This vibrating shape clearly corresponds to the first mode of the sample. The nodal line in the center follows a regular pattern parallel to the edges of the plate, but the antinodal zones exhibit asymmetries between them. This asymmetry may have been associated with the mounting of the sample but had no influence on the presence and shape of the antinodal zones obtained.

Other samples had different graphical evidence, as shown in Figure 3(2,3). In Figure 3(2), the nodal lines are parallel to the edges in the x axis. This was the result of the superposition of propagating bending waves in the sample, which were excited by the external force and, thus, caused resonance patterns. Even though the three node lines generated exhibited evident definition, the zones of maximum displacement did not show this feature. This may have been due to imperfections in the experimental fixture and to some nonlinearities. Therefore, only one antinode was determined because of the greater certainty in its definition.

A sample with different time of exposure and frequency is characterized in Figure 3(3), where two nonparallel node lines can be seen. Even though two well-defined node lines occurred, the antinode zones were not clear. A perfect clamped boundary is difficult to achieve in practice. Any compliance in the boundaries or in-plane compressive stress due to mounting results in some unclear vibration patterns. However, despite this, two antinode zones were defined in regions ensuring two zones of maximum displacement amplitude. In both cases, antinodal lines with different distributions were observed. These variations were directly related to the greater differential pressures applied to the upper and lower edges of both plates and the mounting of the samples and led to the presence of nonparallel nodal lines.

Nevertheless, it should be noted that the discontinuities detected on the PET layer as a result of the resonance applied to the samples, and therefore, as a consequence of the different mode patterns employed and the antinodal areas generated on the
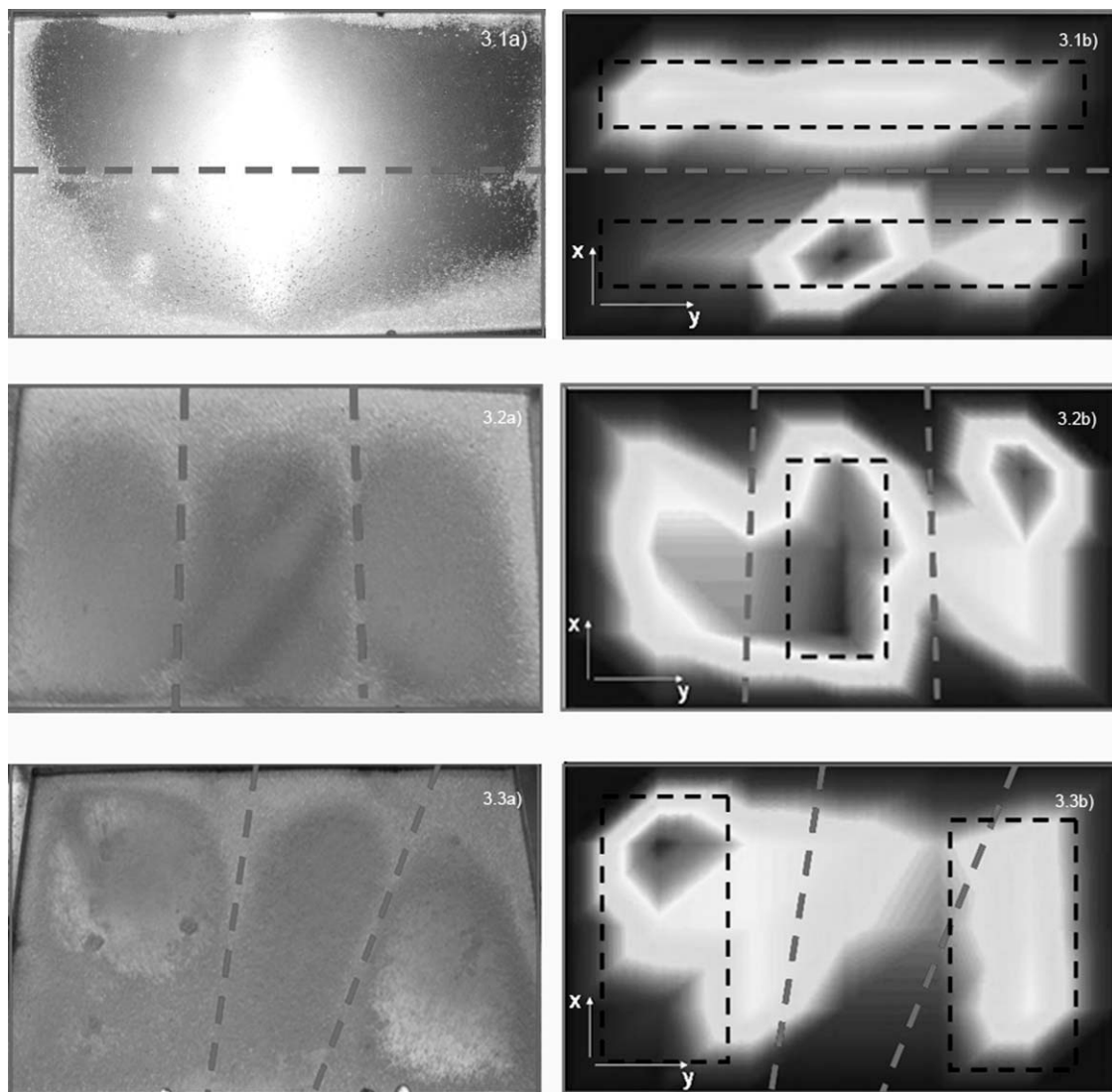
Figure 3   (a) Node line and (b) antinode zone for samples exposed (1) for 1 h to an exciting frequency of 280 Hz, (2) for 3 h to an exciting frequency of 200 Hz, and (3) for 2 h to an exciting frequency of 370 Hz.

PET-coated ECCS samples, this suggests that the adhesion of the PET layer was highly sensitive to the bending waves prevailing in the induced resonance states. The former has important consequences because any linear dynamic state in a given structure can be described as the superposition of different modes of vibration operating together. Thus, any plate's motion pattern governed primarily by bending waves has the potential to generate surface discontinuities on a body, as confirmed by the characterizations and observations of the PET–ECCS composites.

If the excitation force has frequency components corresponding with the resonance frequencies of the body of interest, the main areas of detachment will be found in zones of the greatest deflection or antinodal zones, according to the modal pattern of the body in question. It is still necessary to investigate how this force must be applied to produce damage.

The occurrence of failures, even in samples submitted only for 1 h to resonance conditions, was further evidence of the destructive effect of bending waves on the PET layer of the composites. The practical implications of this fact are important at the industrial level because the longer transit times implied the extended exposure of containers to vibrations and, therefore, a possible risk factor of damage occurrence for the PET layer in contact with food.

When randomly analyzing the antinode zones, we found localized metal–polymer bonding failures, which contributed to the detachment of the layers and showed a different vibration behavior, depending on the intensity of the existing failures. Therefore, a rigorous analysis of the sample tested for 2 h at 370 Hz was made.

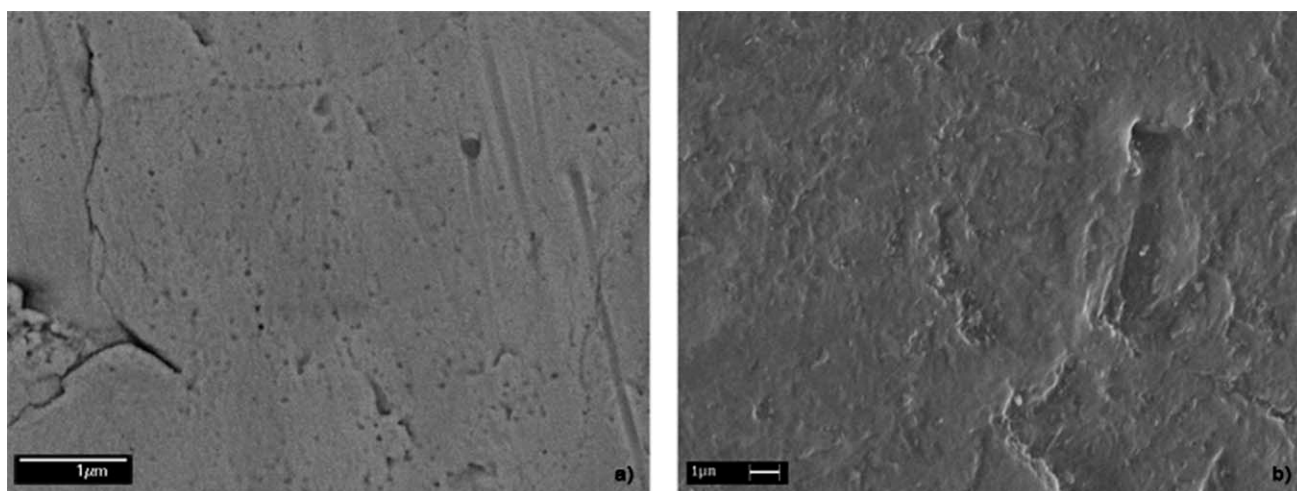Figure 4 shows different types of failures. Figure 4(a) indicates those points where the PET layer did

Figure 4 Morphology of surface defects: (a) specific defects on the chromium protective layer (900×, SEM) and (b) surface defects on the PET layer due to the coextrusion of the colaminate.

not offer complete protection to the electrolytic chromium coating; this exposed it to the environment because of the presence of discontinuities. The dark circular areas represent the unprotected parts of the steel, evidencing failures in the chemical and mechanical bonding of the PET-coated ECCS plate. The localized absence of the chromium oxide layer between the steel plate and the PET coating prevented the formation of chemical bonds, created discontinuities or critical points, which manifested in the presence of vibrations, and at the same time, exposed the antinodes, which led to an unstable behavior of the metal–polymer system. Hence, the manufacturing processes of metal–polymer laminated materials are relevant to their employment as food containers.

On the other hand, surface defects derived from the manufacturing processes, such as colaminating by the coextrusion of the PET coating on the steel plate and mechanical processes of the composite, can be observed in Figure 4(b).

Surface defects of polymers, such as the pores, rugosities, blisters, and bending characterized by electron microscopy, limit their protective capacity, generate discontinuities on the coating, and constitute sensitive points that lead to the failure of composites. Thus, the vibrational tests evidenced the existence of these defects, associated and characterized as antinodal areas, which could progress under long-term vibration conditions, such as during the transportation of these materials.

The cross-sectional characterization of the PET coating, which started from the PET surface until the ECCS interface was reached, was performed by means of D dual beam microscopy. This procedure generated a frontal wall by erosion of the PET coating and showed the presence of the titanium dioxide

(TiO_2) pigments that confer the white color to the polymer in applications such as food containers (Fig. 5). This characterization was important to determine the influence of the TiO_2 pigments on the viscoelastic behavior of the coating material studied and under the resonance conditions imposed. An evaluation of the former indicated that these nanometer-sized particles in the thickness of PET coating did not influence the generation of antinodal areas, which were rather associated with defects in the continuity of the composite's layers and with the quality of the protective polymer surface.

The Raman vibrational spectroscopy analyses of the TiO_2 distribution in the PET coating are shown
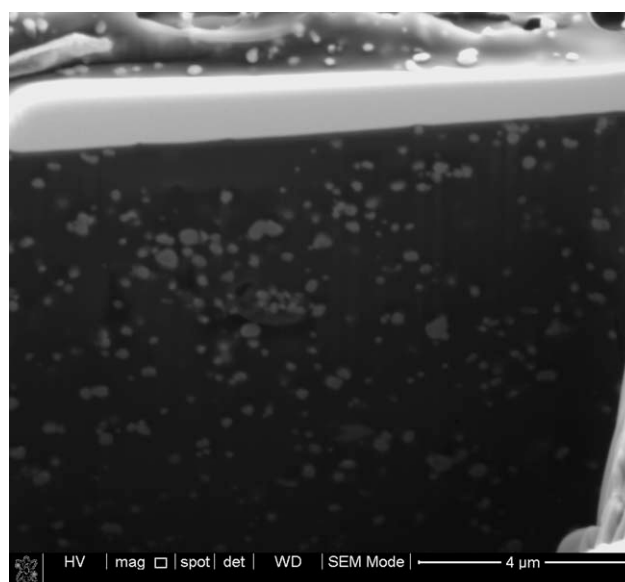

Figure 5 In-depth distribution of TiO_2 particles in the PET coating with sizes ranging from 50 to 500 nm.
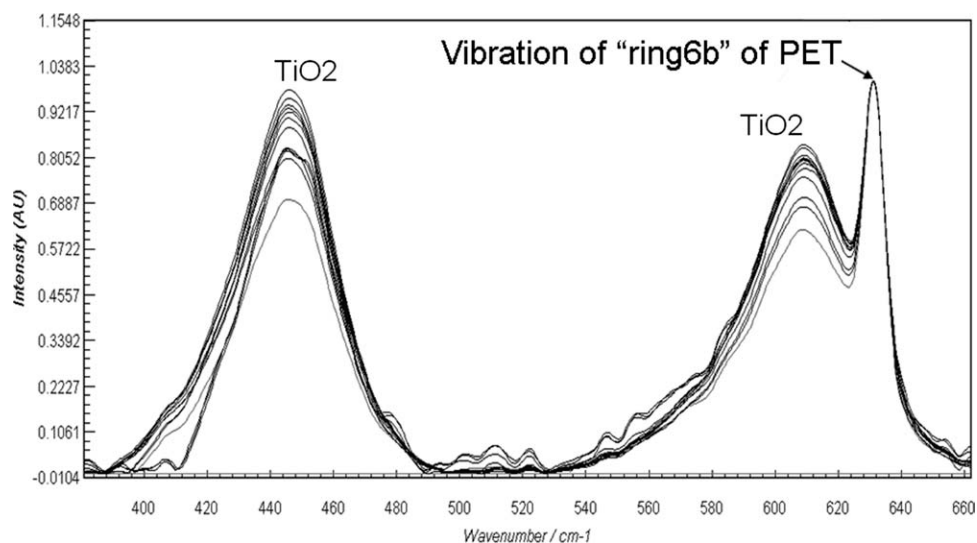
Figure 6 Unit standardization of the intensity of the ring 6b band of the PET coating. The intensities of the rutile show a dependence on the depth.

in Figure 6. We analyzed the samples at parallel intervals by obtaining spectra every 5 μm, starting from the PET surface until reaching the ECCS interface, to determine and verify the presence of rutile in the PET thickness. The intensity of the bands was greater near the polymer surface and decreased toward the metal interface. After the forced vibration tests, the Raman spectra of rutile were all similar from the midpoint of the coating thickness to the surface, with no chemical changes either in composition or orientation in the most significant bands, 444 and 608 cm^{-1}. The spectra showed a correlation with the microstructural observations because the TiO$_2$ pigments reached only half of the thickness of the polymer from the PET surface, which was confirmed in zones with antinodes and without them and whose distribution had no influence on the vibration behavior of the PET-coated ECCS steel composite.

CONCLUSIONS

In this work, a controlled experimental procedure devised to produce surface damage with mechanical vibration resonance in metal–polymer samples has been presented. The experimental setup used for the vibration studies determined zones with antinodes of different natures; these indicated inelastic–elastic behavior instabilities of the composites' substrates associated with physical and mechanical factors of the material.

From the results obtained, it could be concluded that the controlled generation of antinode zones in clamped polymer–metal sheets subjected to forced harmonic vibrations constituted a reliable method to promote the appearance of microscopic failures on the PET surface. The electron microscopy characterization of antinode zones in the samples studied showed differences with respect to homogeneous areas and showed a greater presence of surface defects at the metal–polymer interface level, such as discontinuities of the protective polymer, deformations, microcracks, bending, pores, and exposure points of the metal substrate, due to failures of the polymer coating. A clear relationship between PET delamination and areas of the sheet subjected to greater amplitudes of deformation was established according to the results of the analyses.

On the other hand, the Raman spectroscopy analyses of the TiO$_2$ pigments incorporated into the structure of the PET polymer did not confirm changes in its cross-sectional distribution in the antinode zones; this implied that these pigments did not influence the vibration behavior of the metal–polymer composite.

References

1. Zumelzu, E.; Rull, F.; Schmidt, P.; Boettcher, A. Surf Coat Int B 2006, 89, 57.
2. Schrauwen, B. A. G.; Janssen, R.; Govaert, L.; Meijer, H. E. H. Macromolecules 2004, 37, 6069.
3. Zumelzu, E.; Rull, F.; Boettcher, A. J Mater Process Technol 2006, 137, 34.
4. Cho, C. K.; Kim, J. D.; Park, C. E.; Lee, S. W.; Ree, M. J Adhes Sci Technol 2000, 14, 1131.
5. Zumelzu, E.; Rull, F.; Boettcher, A. Surf Eng 2006, 22, 1.
6. Barilli, E.; Fragni, R.; Gelati, S.; Montanari, A. Prog Org Coat 2003, 46, 91.

7. Zumelzu, E.; Gipoulou, G. Surf Coat Int B 2002, 85, 35.
8. Compararo, D.; Brown, H.; Spinks, G.; Jessop, K. Presented at the 8th International Tinplate Conference, Paris, France, Oct 2004.
9. Zumelzu, E.; Rull, F.; Ortega, C.; Cabezas, C. J Appl Polym Sci 2009, 113, 1853.
10. Arenas, J. P.; Pereira, R.; Zumelzu, E. Presented at the 16th International Congress on Sound and Vibration, Poland, Krakow, July 5–9, 2009.
11. Adhicari, S. Mech Syst Signal Process 2004, 18, 1.
12. Arenas, J. P. J Sound Vib 2003, 266, 912.
13. McRae, J. D.; Naguib, H. E.; Atalla, N. J Appl Polym Sci 2010, 116, 1106.
14. Sorrentino, L.; Di Maio, E.; Iannace, S. J Appl Polym Sci 2010, 116, 27.
15. Lin, C.; Sun, H.; Wang, S.; Huang, J.; Li, J.; Guo, S. J Appl Polym Sci 2010, 116, 320.
16. Cruz, S. A.; Zanin, M.; Nascente, P. A. P.; Bica de Moraes, M. A. J Appl Polym Sci 2010, 115, 2728.
17. Baxi, R. N.; Pathak, S. U.; Peshwe, D. R. J Appl Polym Sci 2010, 115, 928.
18. Chauhan, S.; Karmarkar, A.; Aggarwal, P. J Appl Polym Sci 2009, 114, 2421.
19. Demirel, B.; Daver, F. J Appl Polym Sci 2009, 114, 1126.
20. Li, W.; Schlarb, A. K.; Evstatiev, M. J Appl Polym Sci 2009, 113, 3300.
21. Yin, H.; Yu, D. J Appl Polym Sci 2009, 113, 306.
22. Zhang, S. H.; Chen, H. L. Compos Struct 2006, 74, 63.
23. Hutin, C. Sound Vib 2000, 34, 18.